

Picosecond Time-Resolved Resonance Raman Probing of the Light-Switch States of $[\text{Ru}(\text{Phen})_2\text{dppz}]^{2+}$

Colin G. Coates,[†] Johan Olofsson,[‡] Monica Coletti,[†] John J. McGarvey,^{*,†} Björn Önfelt,[‡] Per Lincoln,[‡] Bengt Norden,[‡] Eimer Tuite,^{*,‡,§} Pavel Matousek,^{||} and Anthony W. Parker^{||}

School of Chemistry, The Queen's University of Belfast, Belfast BT9 5AG, Northern Ireland, Department of Physical Chemistry, Chalmers University of Technology, S-412 96 Gothenburg, Sweden, Department of Chemistry, University of Newcastle upon Tyne, Newcastle upon Tyne NE1 7RU, U.K., Central Laser Facility, CLRC Rutherford Appleton Laboratory, Chilton, Didcot, Oxfordshire OX11 0QX, U.K

Received: July 16, 2001

Picosecond time-resolved resonance Raman (picosecond-TR³) spectroscopy has been used to conduct an extensive photophysical characterization of the “light-switch” complex $[\text{Ru}(\text{phen})_2\text{dppz}]^{2+}$ as a function of environment, in which studies have been carried out in aqueous and nonaqueous media and in DNA. The results are considered in relation to a previous report describing “environment-sensitive” lowest triplet MLCT states. Vibrational marker features and enhancement patterns were used to determine the rapid progression (<20 ps) between two triplet MLCT states in aqueous environment, followed by subnanosecond, nonradiative deactivation to the ground state. In nonaqueous environment, the long-lived, emissive triplet MLCT state is spectrally identified as the short-lived first triplet MLCT state observed in water, in agreement with the earlier proposed mechanism. The present data are shown to correlate well with previous nanosecond RR findings for the complex in each environment. Interestingly, a “precursor state” has been identified upon excitation in both nonaqueous solvent and in DNA, which precedes the triplet MLCT state, and the lifetime of which appears to be environment dependent. Observation of this state is discussed in relation to other recent femtosecond spectroscopic studies on this complex.

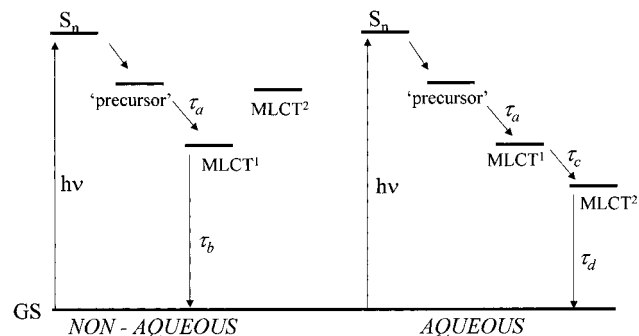
Introduction

The clinical utility of metal complexes which bind to DNA has heightened interest in their spectroscopic and photophysical behavior^{1,2} and a range of techniques has been employed in studying the nature and consequences of the interactions involved, including steady-state, time-resolved and luminescence spectroscopy, linear dichroism,^{1f} transient resonance Raman spectroscopy,^{1o,p} NMR,^{1l} and gel electrophoresis.^{1e}

The “light-switch” complex $[\text{Ru}(\text{L})_2\text{dppz}]^{2+}$ (L = 1,10-phenanthroline (phen), 2,2'-bipyridine (bpy); dppz = dipyrido-[3,2-*a*:2',3'-*c*]phenazine) has been of particular interest over recent years, due to the marked luminescence enhancement which it undergoes upon intercalation of the dppz ligand within the base pairs of double-^{1a,d,e,k} and single-stranded nucleic acid.³ This intriguing responsiveness of the dppz ligand to the local “solvent” environment has prompted a number of studies into both the detailed mode of binding of the complexes to DNA,^{1d,k} and the factors responsible for the luminescent properties of the complex, to establish the mechanism for the light-switch response.^{4,5}

On the basis of a recent investigation into the photophysical response of the complex $[\text{Ru}(\text{phen})_2\text{dppz}]^{2+}$ to solvent environment, employing picosecond time-resolved luminescence and absorption techniques, Barbara et al. proposed a possible mechanism of the light-switch effect.⁴ The model involves two close-lying MLCT states⁶ of triplet character—MLCT¹ and

SCHEME 1



S_n —singlet state manifold accessed by initial light absorption.

τ_a varies with solvent environment—see text.

τ_b is typically several hundred nanoseconds (radiative).^{1,4,5}

τ_c is ca. 5–10 ps—see text.

τ_d is ca. 250 ps (non-radiative).

MLCT²—the relative energies of which are sensitive to the polarity of the solvent environment (see Scheme 1).⁷ Both the proposed MLCT states are “dppz-based”, formally $[\text{Ru}^{\text{III}}(\text{phen})_2(\text{dppz}^-)]^{2+}$. In water, it was proposed that decay following excitation progresses rapidly (~3 ps) through MLCT¹ to MLCT² from which a largely nonradiative, rapid (250 ps) decay to ground-state ensues. In a less polar solvent, such as acetonitrile, it was suggested that the MLCT² state lay sufficiently high in energy relative to MLCT¹, that intense luminescent decay from the MLCT¹ state became the dominant process. Murphy et al. have reported studies examining steady-state and time-resolved luminescence spectra of **1** in a series of nonaqueous solvents.⁵

[†] School of Chemistry.

[‡] Department of Physical Chemistry.

[§] Department of Chemistry.

^{||} Central Laser Facility.

An investigation by femtosecond TA of **1** together with two structurally related complexes of Ru(II) has also been reported recently by the Gothenberg group.⁸

We have earlier described detailed resonance Raman (RR) and nanosecond excited-state resonance Raman investigations, probing the nature of the excited state of $[\text{Ru}(\text{phen})_2\text{dppz}]^{2+}$ (**1**) and its interaction with nucleic acid.¹⁰ Such methods are particularly effective for identifying the structure of the excited states of transition metal and organometallic complexes⁹ and have indeed provided a powerful spectroscopic handle for studying the present system.¹⁰

The present investigation presents a detailed account of picosecond TR³ studies into the photophysical nature of **1** in solvent environments of varying polarity and when complexed with DNA. Significant spectroscopic and kinetic evidence is provided which supplements our previous nanosecond excited state RR studies and is now considered here in relation to the recently proposed scheme by Barbara et al., that the light-switch mechanism involves two "solvent-responsive" charge-transfer states. In addition, a short-lived, also solvent-dependent precursor state has been detected, which is more prominent (on this time-resolution) in less polar environments than in aqueous solution, but does not appear to play any direct role in the light-switch mechanism. The results are also considered in parallel with recent time-resolved picosecond transient absorption studies of **1** conducted by the Belfast group in various solvent environments, alongside the recent femtosecond TA study.⁸

Experimental Section

Chemicals. $\text{RuCl}_3 \cdot x\text{H}_2\text{O}$, d_3 -acetonitrile, d_4 -methanol, and calf thymus (CT) DNA were obtained from commercial sources (deuterated solvents were necessary to shift strong solvent peaks away from the spectral region of interest to facilitate the location of key features in both ground and excited-state RR spectra). Literature methods were used for the preparation of racemic $[\text{Ru}(\text{phen})_2\text{dppz}]\text{Cl}_2$.^{1d} All picosecond-TR³ measurements were made on solutions which were ~ 1 mM in metal complex; nanosecond excited-state RR measurements were made on $\sim 10^{-4}$ M solutions. DNA concentration is expressed in terms of bases and was determined by absorption spectroscopy using $\epsilon_{260\text{ nm}} = 6600\text{ M}^{-1}\text{ cm}^{-1}$. CT DNA was dissolved in a buffer 5 mM sodium phosphate (pH 6.9)/100 mM NaCl to a concentration of ca. 15 mM and sonicated on ice with an ultrasonic probe using 2 s on/2 s off pulses for a total of 8 min. The sonicated DNA was then centrifuged at ca. $700 \times g$ for 20 min, and finally passed through a Whatman Hepa-vent filter to remove aggregated material. Comparison of the mobility of the sonicated DNA with a molecular weight ladder on a 1% agarose gel, revealed a polydisperse sample of ca. 100–1000 bp length. Sonication substantially reduced the viscosity and the sonicated DNA was suitable for use in the jet at concentrations of up to ca. 10 mM bases.

Instrumentation. The ultrafast TR³ setup at RAL has been described in detail elsewhere.¹¹ Briefly, the picosecond-TR³ apparatus uses a regenerative amplifier system providing a 1 ps, 800 nm pulse (0.2 to 0.7 mJ), which is frequency doubled to pump an optical parametric amplifier (OPA) generating a probe pulse at 1 kHz.

Two combinations of pump and probe pulses with pulse duration of 1 ps were employed: 400 nm pump/350 nm probe, (pulse energies 10 and 3 μJ , respectively), and 390 nm pump/390 nm probe (10 μJ each). Each pulse had a spot diameter of $\sim 300\text{ }\mu\text{m}$ at the sample. The 400/350 nm combination was used without a Kerr gate (see below) but with a Tripletmate three-

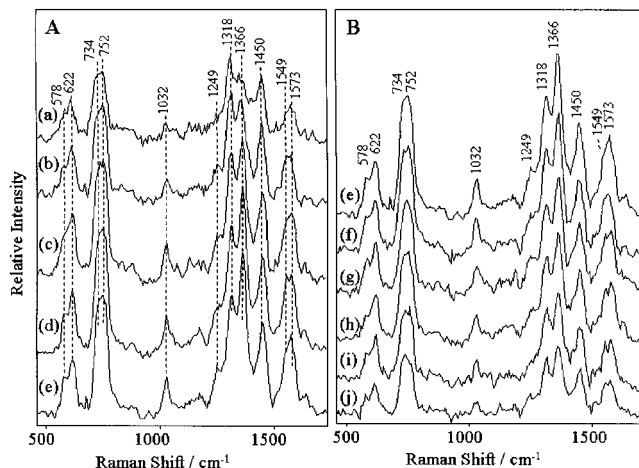


Figure 1. Pure excited-state picosecond-TR³ spectra of **1** in water at 390 nm pump/390 nm probe time delays of (a) 4, (b) 7, (c) 10, (d) 20, (e) 30, (f) 50, (g) 80, (h) 130, (i) 180, and (j) 230 ps. A: first phase of decay. B: second phase of decay.

stage spectrometer in place. The 390/390 nm combination was used with the Kerr gate in order to eliminate Raman signal from the pump pulse. A single-stage spectrometer in combination with a supernotch filter was employed with this particular arrangement. The picosecond-TR³ signal was collected at 90° geometry, dispersed through a spectrograph and detected by a liquid nitrogen cooled CCD. The pump and probe beams were polarized in parallel.

The Kerr gate¹² was developed fundamentally for efficient rejection of fluorescence from Raman signals, the fast gating arising from induced transient anisotropy of a CS_2 Kerr medium, in a 2 mm cell, driven by a residual 800 nm laser pulse (1 ps, 500 μJ), focused to a 1–2 mm diameter spot, with a gating time of ~ 4 ps (fwhm). The requirement of the gate in the current investigation however was not so much to reduce background fluorescence, as to enable the use of a single wavelength (390 nm) pump–probe arrangement by eliminating the Raman signal arising from the pump beam. For pump–probe delay times of 4 ps, it was necessary to subtract a spectrum recorded of pump only at the corresponding time delay to correct for "leakage" through the Kerr gate of Raman signal arising from the pump.

A vertically flowing open jet (500 μm diameter) sample arrangement was employed, requiring sample volumes of the order of 20 mL.

Nanosecond excited-state resonance Raman spectra were generated by the well-known single-color pump and probe method,¹⁰ in which the leading edge of the laser pulse incident on the sample pumps the molecules into the excited state and the trailing edge probes the Raman scattering. Samples were contained in spinning cells in order to minimize the possibility of thermal degradation and/or photodegradation, especially where relatively long spectral accumulation times (10–15 min) at a pulse repetition rate of 10 Hz were required to obtain signals of good quality. The transient spectra were recorded with a multichannel detector (EG&G OMA III with Model 1420B intensified detector) coupled to a triple spectrometer of simple, in-house design, described earlier.¹³ Incident pulse energies were typically ~ 3 mJ.

Results

$[\text{Ru}(\text{phen})_2\text{dppz}]^{2+}$ in Aqueous Environment. Figure 1 shows the picosecond-TR³ spectrum of **1** in water recorded with both pump and probe beams at 390 nm. The Kerr cell technique

was implemented for this wavelength combination in order to exclude collection of Raman signal from the pump beam. With CS_2 as the Kerr medium, the minimum pump–probe delay was limited to 4 ps, below which significant leakage of pump signal occurred through the Kerr gate setup. The spectra shown above, recorded over pump–probe delays ranging from 4 to 230 ps, have each been corrected for scattering by ground-state species through careful subtraction of the spectrum obtained at -20 ps, scaled for removal of the known ground-state feature at 1409 cm^{-1} . This proved to be a very effective method of obtaining spectra representative of the pure excited-state species at each time delay and was used throughout the investigation. In general, the spectra shown display features which are in good agreement (bearing in mind the larger bandwidth of ultrafast vibrational spectra) with excited-state spectra of **1** in water from previous single-color RR studies, recorded with 396 or 355 nm laser pulses of approximately 8 ns duration.¹⁰ From such studies, through comparison with spectra of the complexes $[\text{Ru}(\text{bpy})_2\text{dppz}]^{2+}$, $[\text{Ru}(\text{dppz})_3]^{2+}$, and $[\text{Ru}(\text{phen})_3]^{2+}$, features at ca. 1575, 1545, 1455, 1366, 1316, and 1261 cm^{-1} have been attributed to vibrations of the radical anion of dppz ($\text{dppz}^{\cdot-}$) of the triplet MLCT state (formally $[\text{Ru}^{\text{III}}(\text{phen})_2(\text{dppz}^{\cdot-})]^{2+}$, in resonance with $\pi^*-\pi^*$ transitions of the $\text{dppz}^{\cdot-}$ ligand. Ancillary phen vibrations contribute at ca. 1630, 1581, 1512, 1455, and 1309 cm^{-1} . Further studies^{14a,b} with deuterated analogues of **1** have enabled the “regional assignment” of dppz vibrations in the ground and excited-state species as modes which are localized either on “phenanthroline” or “phenazine” segments of the dppz ligand, or are more delocalized in character.

The series of spectra in Figure 1 can be seen to encompass two distinct decay phases, following excitation. A first phase, shown in Figure 1A is apparent over the approximate time range 4–20/30 ps, exhibiting a grow-in of the $\text{dppz}^{\cdot-}$ 1366 cm^{-1} feature, relative to neighboring $\text{dppz}^{\cdot-}$ peaks, e.g., 1318 cm^{-1} , an increase in absolute intensity of all of the features occurring across the spectrum. This observation corresponds to grow-in of a state which, as will be shown later, can be identified with that labeled MLCT^2 in the mechanism in Scheme 1. The second series of spectra, recorded at longer pump–probe delays (Figure 1B) is characterized by a general reduction in intensity of the excited-state features over the time scale 30–230 ps. To derive kinetic information from the spectra, a series of subtractions was performed, shown in Figure 2A, in which each of the early time spectra was subtracted from the spectrum recorded at 130 ps (taken to mark the time by which conversion to the second state is essentially complete). The resulting subtracted spectra reveal the difference in spectral enhancement pattern between the early and later states, indicating that (a) the 1366 cm^{-1} feature does indeed exhibit the largest difference in relative intensity, but with lower intensity features growing also at ca. 628, 744, 1464, and 1579 cm^{-1} in the spectrum of the second state, and (b) interstate conversion is virtually complete by 20 ps, with no evident difference in enhancement pattern at times later than this. This is well illustrated by the plot vs time in Figure 2B of the intensity of the 1366 cm^{-1} feature.

Spectra of **1** in aqueous environment recorded with pump and probe beams set at 420 nm, again making use of the Kerr gate, are shown in Figure 3A. The traces were recorded over a range of pump–probe time delays spanning 4 to 550 ps. As observed for the studies at 390 nm, an initial growth in the relative intensities of several features is observed, followed by depletion across the spectral range, over the time delays probed, analogous to that observed in Figure 1. In addition, a kinetic plot derived from the relative intensity of the 1366 cm^{-1} feature

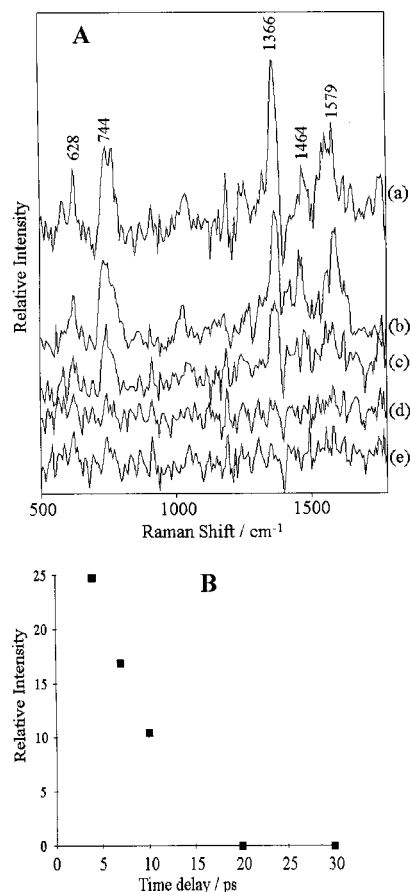


Figure 2. A: subtraction spectra of **1** in water at 390 nm pump/390 nm, derived from pure excited-state spectra of Figure 1 (a) = 130–4 ps, (b) = 130–7 ps, (c) = 130–10 ps, (d) = 130–20 ps, and (e) = 130–30 ps. B: Kinetics derived from A, plotting relative intensity of 1366 cm^{-1} feature vs time delays between 4 and 30 ps.

in the spectra of Figure 3A, is shown in Figure 3B. A grow-in is evident between 4 and 20 ps, followed by an exponential decay with a time constant ca. 250 ps.

Figure 4 shows a further series of pure excited-state spectra of **1** in water, but in this case recorded with a 400 nm pump and 350 nm probe combination (without the Kerr cell, which was regarded as unnecessary with this wavelength combination), at a range of time delays between 0 and 200 ps. As for the spectra recorded at a probe wavelength of 390 nm, bands appear at similar positions to those recorded in earlier single-color RR experiments with 8 ns pulses at 355 nm. Figure 4A shows excited-state spectra, from which it is evident that an overall growth in relative band intensities takes place over the shorter time delays. While the apparent spectral intensities at the shortest delay times will be influenced by the cross-correlation time of the two laser pulses, further intensity increases clearly occur beyond 4 ps. The overall kinetic picture is shown in Figure 6A, derived from measurement of the intensity of the 1366 cm^{-1} feature at each time delay between 0 and 200 ps. A significant grow-in occurs over the first 20 ps, in good agreement with the early time kinetics derived from the studies at 390 and 420 nm, followed by a longer-lived decay. Figure 4B shows the same excited-state spectra over the 0–200 ps time delay range, with the intensities normalized to the 1366 cm^{-1} feature, to study the changes in enhancement pattern over time. The feature near 1570 cm^{-1} is noteworthy. It is most likely a combination of bands, which can be compared to those observed at 1545, 1575, and 1600 cm^{-1} in the nanosecond spectra of **1** in water. It is

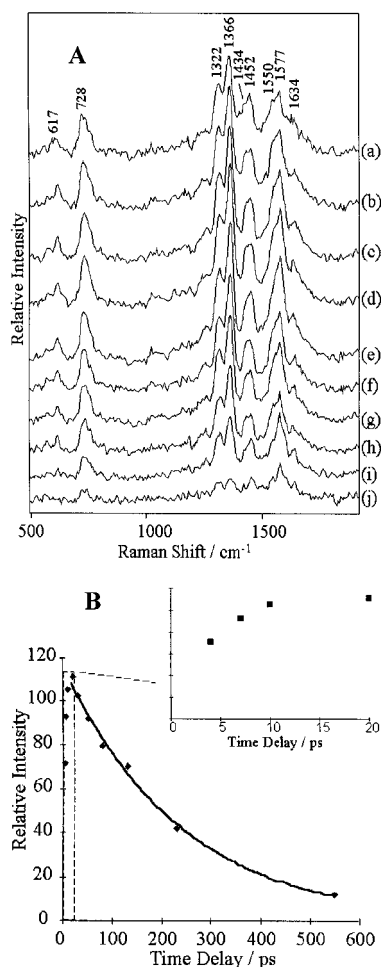


Figure 3. A: pure excited-state picosecond-TR³ spectra of **1** in water at 420 nm pump/420 nm probe time delays of (a) 4, (b) 7, (c) 10, (d) 20, (e) 30, (f) 50, (g) 80, (h) 130, (i) 230, and (j) 550 ps. B: kinetics derived from A, plotting relative intensity of 1366 cm⁻¹ feature vs time delays between 0 and 550 ps. Inset: expanded kinetics between 0 and 20 ps.

evident from Figure 4B that a marked shift of this composite band to higher frequencies occurs, with increasing time delay.

To try to establish the origin of this shift, spectra recorded at later times were subtracted from those at earlier. One such subtraction in Figure 5A shows the result of subtracting the 100 ps spectrum from the 2 ps spectrum, scaled for removal of the 1366 cm⁻¹ peak. Significantly, a strong feature is apparent at 1526 cm⁻¹, evidently paralleling the 1526 cm⁻¹ feature previously reported¹⁰ in our nanosecond investigations and attributed as a marker band of the ³MLCT state of the complex which is dominant in nonaqueous environments (i.e., DNA or acetonitrile). It should also be noted that there are other features present in the subtraction spectrum, pointing to further differences in the enhancement patterns, possibly indicating that two states are probed at this wavelength. For comparison, Figure 5B shows nanosecond single-color excited-state spectra recorded of **1** in acetonitrile and aqueous environments with a 355 nm excitation pulse. Subtraction of the spectrum recorded in water from that in acetonitrile yields a spectrum which not only exhibits a strong 1526 cm⁻¹ feature but also some additional bands, albeit less well-defined (given the invariably poorer signal quality of the spectra recorded in acetonitrile), which can be approximately correlated with the subtraction spectrum derived from the picosecond data (Figure 5A).

Kinetic information was again derived from the spectra through a series of subtractions. In this case the pure excited state spectrum for the 100 ps delay time, (taken to represent complete conversion to the second MLCT state), was subtracted from the spectra at each of the early time delays between 0 and 30 ps. The relative intensity of the 1526 cm⁻¹ feature was measured and is plotted against time in Figure 6B, from which it is apparent that conversion to the second MLCT state is complete within some 20 ps after excitation, in good agreement with the kinetics derived earlier from the subtractions of spectra recorded at a probe wavelength of 390 nm (shown also in Figure 6B, for comparison). The finite rise time in the plot in Figure 6A, evident between 0 and 4 ps, can be accounted for in terms of the measured cross-correlation time of the pump and probe pulses.

[Ru(phen)₂dppz]²⁺ in Nonaqueous Environment. To investigate the photophysics in nonaqueous environments, spectra were recorded of **1** in *d*₄-methanol and *d*₃-acetonitrile. For example, Figure 7B shows pure excited-state spectra of **1** in methanol (after subtraction of the -20 ps spectrum), recorded with a 390/390 nm pump-and-probe combination at a range of time delays between 4 and 1000 ps. Importantly, the kinetic behavior of the spectra is distinct from that observed for the complex in water at this probe wavelength. In this case, there is no clear evidence of decay from a second state after 20/30 ps, in contrast to the situation in water. However, closer examination of the spectra reveals additional features, in particular a band near 1390 cm⁻¹. A similar situation arises for the complex in acetonitrile (Figure 7A). At later time delays, this band depletes and there is a concomitant grow-in at 1366 cm⁻¹. It is significant that this change is also accompanied by a grow-in of a band at ca. 1526 cm⁻¹. Subtraction of the spectrum recorded at 10 ps from that at 400 ps for both solvent media (upper traces in Figure 8A,B) brings out a number of features, but most significantly those near 1366 and 1526 cm⁻¹, the latter band being more evident in the case of the CD₃OD spectra. The outcome of spectral subtraction in the reverse order (i.e., 10–400ps) is shown in the lower traces in Figure 8. It should be stressed that the function of subtraction here is to highlight the *differences* between the spectra of the early and later states, and should not be interpreted as representing pure excited state spectra of the respective states. Although the results are noisy, the bands which emerge display some important differences from those in the upper traces, particularly the feature near 1390 cm⁻¹, present for both solvents, but more distinct in CD₃OD. The appearance in the subtracted spectra of the features near 1390 and 1366 cm⁻¹ at different stages of the decay is significant, especially in relation to another recently published study¹⁵ of the excited state of the 2,2-bipyridyl analogue of **1**, [Ru(bpy)₂dppz]²⁺. This point is considered in the Discussion, below.

Also shown in Figure 9 are some spectra of **1** bound to CT-DNA (*P/D* = 8.5), recorded with the same pump–probe wavelength combination. Although the three delay times shown provide some indication of subtle changes in the intensity ratio of (1390 cm⁻¹)/(1366 cm⁻¹) similar to those observed in MeOD and CD₃CN, they are on the borderline of being detectable above the noise and we do not wish to overinterpret them. However, the signal appears to grow in over the 100 ps range studied. Similar observations were made for samples with *P/D* values of 5 and 10.

Spectral changes in the presence of DNA become more evident when the probe wavelength is altered to 420 nm. Figure 10 shows pure excited-state picosecond-TR³ spectra of **1** in

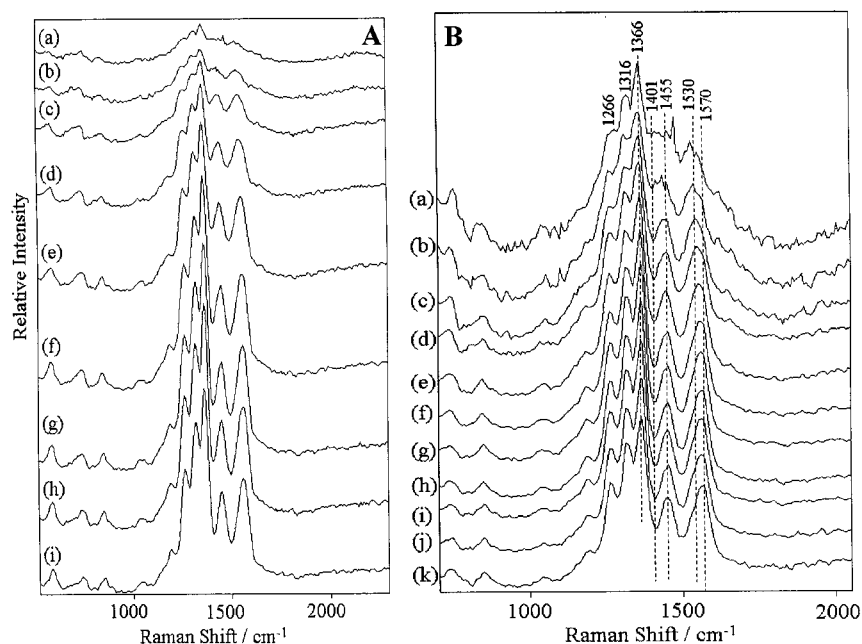


Figure 4. A: pure excited-state picosecond-TR³ spectra of **1** in water at 400 nm pump/350 nm probe time delays of (a) 0, (b) 1, (c) 2, (d) 4, (e) 6, (f) 10, (g) 20, (h) 30, and (i) 50 ps. A: true relative intensity of spectra. B: spectra normalized to intensity of 1366 cm⁻¹ band to display transient profile. (Traces in A at time delays of 100 and 200 ps deleted for clarity of presentation).

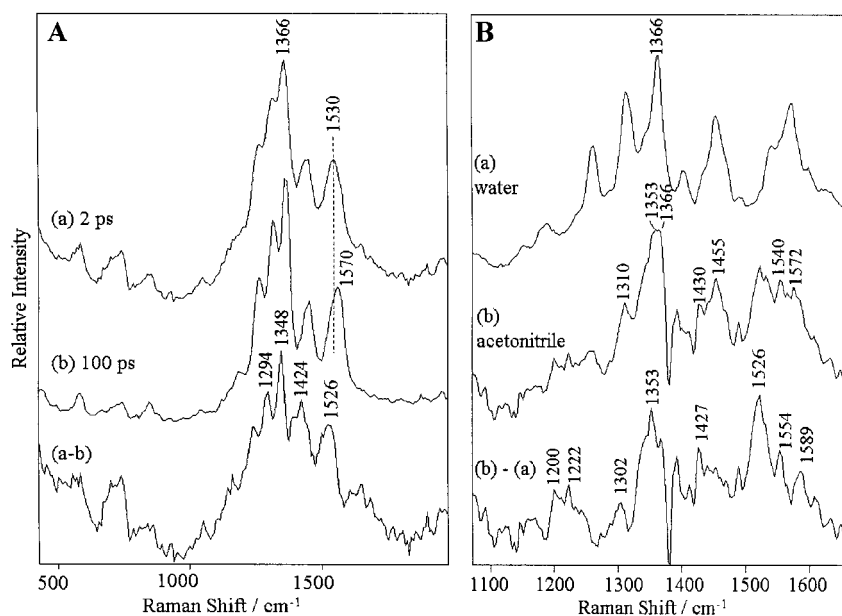


Figure 5. A: spectra exhibiting the difference in transient profile with time of **1** in water at 400 nm pump/350 nm probe; (a) 2 ps, (b) 100 ps, (a - b) subtraction spectrum 2–100 ps. B: Excited-state nanosecond RR spectra of **1** at $\lambda_{\text{ex.}} = 355$ nm in (a) water, (b) acetonitrile (subtracted), and (b - a) subtraction spectrum.

nonaqueous environments, recorded with a 420/420 nm pump and probe combination. Figure 10A, in acetonitrile solvent, is spectrally similar to that observed with the 390 nm probe in the same environment (Figure 7A), exhibiting a feature at ca. 1390 cm⁻¹, which appears with slightly more prominence at earlier times. Figure 10B was recorded for the complex bound to calf thymus DNA. Although the spectra are generally weaker (due to depletion of dppz⁻ features with respect to neutral phen features because of perturbation to electronic transitions through intercalation¹⁰), a feature can again be identified at ca. 1390 cm⁻¹ alongside the feature at ca. 1366 cm⁻¹ (characteristic of MLCT¹ and MLCT²), suggesting the possibility that at early times the same state may be occupied in acetonitrile and DNA.

Figure 11 shows pure excited-state spectra (after subtraction of the spectrum recorded at -20 ps) of **1** in acetonitrile (A)

and methanol (B), recorded this time with a 350 nm probe, following excitation at 400 nm, at a range of time delays between 0 and 500 ps. It is readily apparent that the spectra at very early times (ca. 0–6 ps) are dominated largely by noise, after which features begin to grow in. The most prominent of the bands which do appear are at 1364, 1449, and 1526 cm⁻¹ and correspond closely to those which had previously been observed in acetonitrile in nanosecond single-color RR studies using 355 nm excitation and attributed to the charge-transfer state now identified here (vide supra) as MLCT¹. This trend in the spectra over very short times is clearly distinct from that seen for the complex in water on short picosecond time scales, using the same pump and probe wavelength combination (Figure 4). Whereas in water the 1526 cm⁻¹ band appears at very early times and then rapidly decays, marking conversion to another

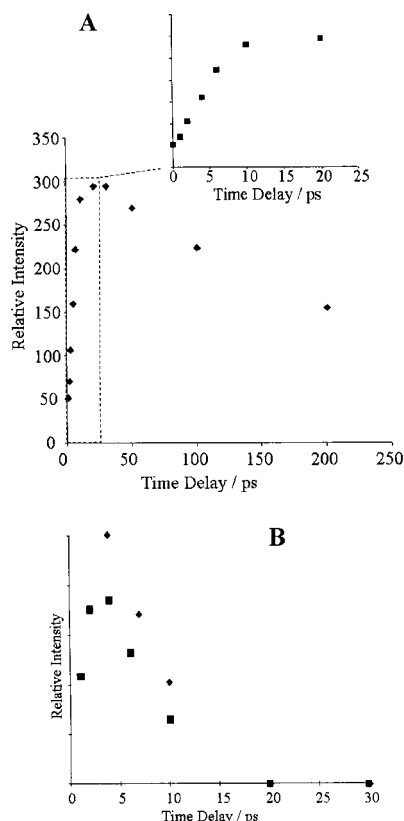


Figure 6. A: kinetics of **1** in water at 400 nm pump/350 nm probe, derived from Figure 4A, plotting relative intensity of 1366 cm^{-1} feature vs time delays between 0 and 200 ps; Inset — Expanded kinetics between 0 and 20 ps. B: (■) kinetics of **1** in water, derived from spectral subtractions analogous to that in Figure 5A, performed for 0–100 ps, 1–100 ps, 2–100 ps, 4–100 ps, 6–100 ps, 10–100 ps, 20–100 ps, and 30–100 ps. Relative intensity of 1526 cm^{-1} feature plotted vs time delays between 0 and 30 ps. (◆) Overlaid kinetics of Figure 2B (390 nm/390 nm subtractions) for comparison.

state, grow-in of a strong 1526 cm^{-1} feature occurs only at later times in acetonitrile (beyond 6ps) and does not decay appreciably within the time range covered. Such observations suggest that the early short-lived state in water is actually the dominant state in acetonitrile.¹⁶

Figure 12 A and B shows kinetic plots derived from the series of spectra in Figure 11 for **1** in acetonitrile (Figure 11A) and methanol (Figure 11B) solvents, each data point derived by measuring the relative intensity of the band at 1364 cm^{-1} . The plots indicate that the rate of grow-in of the MLCT^1 state, which causes resonance at this probe wavelength, appears slightly slower in the case of methanol.

Discussion

Previous studies by the Belfast group¹⁰ have established the utility of the nanosecond TR^2 technique for studying the interactions of the MLCT excited states of both $[\text{Ru}(\text{phen})_2\text{dppz}]^{2+}$ and $[\text{Ru}(\text{bpy})_2\text{dppz}]^{2+}$ with calf thymus DNA, employing excitation wavelengths within the region of strong excited-state absorption between ca. 300–400 nm. For example, spectra recorded using 354.7 nm excitation showed that (a) in the presence of DNA, the intensities of several features assignable to the dppz^- entity of the state ($[\text{Ru}^{\text{III}}(\text{phen})_2(\text{dppz}^-)]^{2+}$ for **1**, decreased with respect to bands of the ancillary (phen) ligands, and (b) subtraction of the spectrum recorded in buffer from that recorded in the presence of DNA yielded a spectrum consisting mainly of neutral ligand vibrations, but also containing a

prominent feature at 1526 cm^{-1} . Observation (a) was attributed¹⁰ to perturbation of the $\pi^*-\pi^*$ transitions of dppz^- due to π -stacking of the ligand within the base pairs of DNA. Observation (b) in the same DNA environment of the prominent feature at 1526 cm^{-1} was attributed to resonance with a transition of dppz^- which is distinct from the dppz^- transitions enhanced in aqueous media alone. Importantly, this feature at 1526 cm^{-1} also appeared prominently in the TR^2 spectrum recorded of **1** in acetonitrile. Since complex **1** is emissive in the latter environment as well, with the same triplet MLCT state involved as in DNA, we were led to the conclusion that the 1526 cm^{-1} feature is in itself a “marker” band or signature for the light-switch effect. It is tempting to take the observation of a distinct “state” a stage further and make the association with the states proposed in the mechanism originally put forward by Barbara et al., based on their picosecond luminescence and single-channel transient absorption studies. The dppz^- feature at 1526 cm^{-1} could reasonably be associated with the MLCT^1 state, the dominant, highly emissive state, which is stabilized in a nonaqueous environment (including DNA) relative to MLCT^2 . In water, the MLCT^1 state is proposed to undergo rapid (ca. 3 ps) internal conversion to a lower-lying MLCT^2 state, possibly via a step which involves formation of a hydrogen bond. The nonradiative return from this state back to the ground state was observed to occur over ca. 250 ps,^{4,8} and is the state which is most likely probed by the single color nanosecond TR^2 technique at 355 nm. Consistent with this, the recorded TR^2 spectra in water lack a 1526 cm^{-1} feature.

Important parallels can be drawn between the nanosecond and picosecond data, the current picosecond studies consolidating the proposals based upon the nanosecond time scale measurements above, and providing convincing evidence of the progression through states. In addition, some more detailed insight is afforded into the photophysical behavior of **1** in solvent environments of varying polarity.

$[\text{Ru}(\text{phen})_2\text{dppz}]^{2+}$ in Aqueous Environment. The series of excited-state spectra in Figure 1, recorded using a 390/390 nm pump and probe combination, clearly represent two phases of decay following excitation. The increase in intensity of the 1366 cm^{-1} feature during the first phase A, shown from the kinetic plot (Figure 2B) to occur over approximately 10–20 ps, can be correlated with previous nanosecond transient RR studies recorded with 396 nm excitation which showed a markedly larger intensity of this 1366 cm^{-1} feature in water compared to acetonitrile.¹⁴ Thus, it may be initially proposed from the earlier series of nanosecond investigations that single color RR studies of **1** in water interrogate the MLCT^2 state, the 8 ns duration pulse creating a pseudo steady-state population of this subnanosecond species from which resonance Raman scattering is probed by the trailing edge of the laser pulse, whereas **1** in an acetonitrile environment yielded a spectrum of MLCT^1 , from which the picosecond- TR^3 spectra described above suggest that there is no further decay to MLCT^2 .

The kinetic plot derived from the data (Figure 2B) indicates a time constant for the conversion between MLCT^1 and MLCT^2 qualitatively in agreement with (though somewhat longer than) the 3 ps proposed by Barbara et al. For the data in aqueous media, the spectral subtractions described above (Figs. 2,3) are useful in establishing that there are no more than two phases of decay in operation beyond 4 ps, within the time-range studied, with no further difference in enhancement pattern between excited-state spectra being evident beyond ca. 20 ps.

This kinetic picture is confirmed by the results of the experiments conducted with a 420/420 nm pump and probe

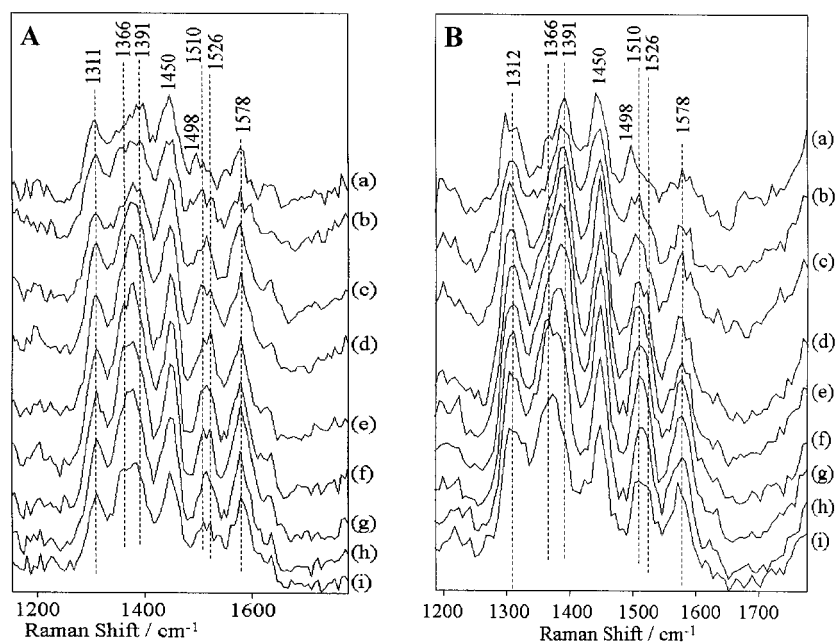


Figure 7. A: pure excited-state picosecond- TR^3 spectra of **1** in d_3 -acetonitrile at 390 nm pump/390 nm probe time delays of (a) 4, (b) 7, (c) 10, (d) 20, (e) 50, (f) 100, (g) 200, (h) 400, and (i) 1000 ps. B: pure excited-state picosecond- TR^3 spectra of **1** in d_4 -methanol at 390 nm pump/390 nm probe time delays of (a) 4, (b) 7, (c) 10, (d) 20, (e) 30, (f) 40, (g) 50, (h) 100, and (i) 400 ps.

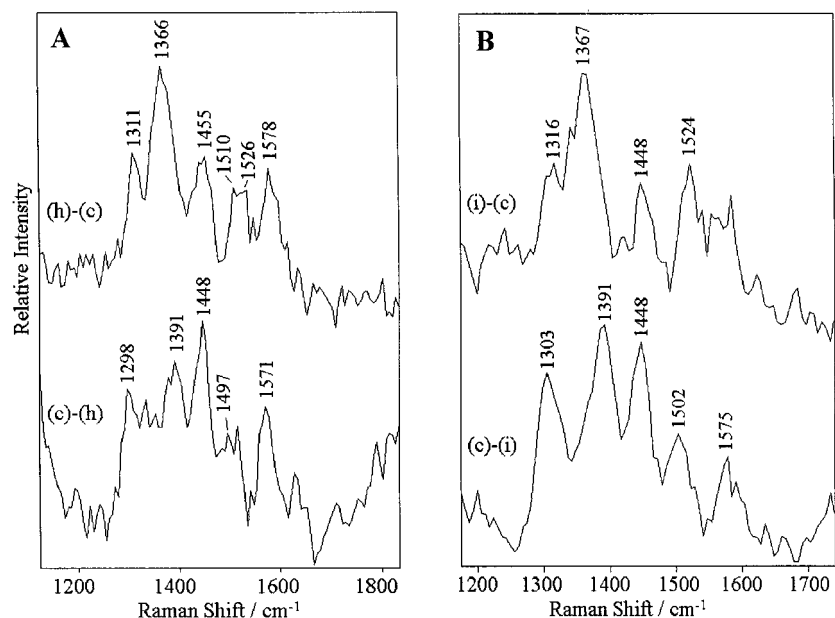


Figure 8. A: subtraction spectra, derived from Figure 7A, exhibiting the difference in transient profile with time of **1** in d_3 -acetonitrile at 390 nm pump/390 nm probe; (h)-(c) = 400–10 ps and (c)-(h) = 10–400 ps. B: subtraction spectra, derived from Figure 7B, exhibiting the difference in transient profile with time of **1** in d_4 -methanol at 390 nm pump/390 nm probe; (i)-(c) = 400–10 ps and (c)-(i) = 10–400 ps.

combination, with the plots shown in Figure 3 again displaying two clear phases of decay, closely related to those observed in the 390/390 nm studies. The first phase can be readily associated with grow-in of the MLCT^2 state, which is complete by ca. 20 ps, directly followed by exponential decay from this excited-state back to the ground state. The time constant estimated from the latter trace is consistent with the value of 250 ps reported by Barbara et al. for the lifetime of the MLCT^2 state. The resonance Raman enhancement pattern of the MLCT^2 excited-state spectra at a probe wavelength of 420 nm is similar to that probed at 390 nm, with perhaps more contribution from neutral phen features. As in the case of the studies using the 390/390 nm pump and probe combination, appropriate subtractions showed that the enhancement pattern exhibited slight changes

over the shortest pump–probe delay times, up to ca. 20 ps, in line with the crossover between states.

Before considering the picosecond TR^3 data recorded with a 350 nm probe, it should be remarked that previous nanosecond RR investigations have shown that probe wavelengths at 396 nm and 355 nm resulted in markedly different enhancement patterns of the dppz^- modes, clearly indicative of more than one transition of dppz^- within the region of strong transient absorption between 300 and 400 nm,¹⁰ in resonance at these probe wavelengths.

The marked grow-in of spectral intensity shown in Figure 4A extends to times beyond the cross-correlation time of the pump and probe pulses (ca. 3 ps), as shown in the kinetic plot derived from the data (Figure 6A) and in fact grow-in is not

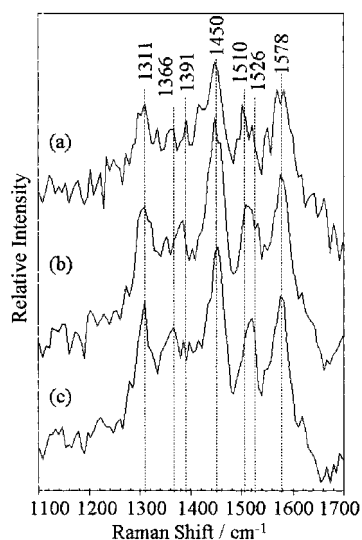


Figure 9. Pure excited-state picosecond-TR³ spectra of **1** with DNA, [DNA phosphate]:[Ru] ratio of 10:1, at 390 nm pump/390 nm probe time delays of: (a) 4, (b) 20, (c) 100 ps.

complete until ca. 20 ps, in excellent agreement with grow-ins derived from the studies at 390 and 420 nm, and attributed to the formation of MLCT.² Thus, it may be supposed that MLCT¹, which is expected to contribute more in the initial stages following excitation in water, is relatively less enhanced at a probe wavelength of 350 nm. This correlates very well with nanosecond TR² studies of **1** at 355 nm as the probe and excitation wavelength, in which it has been observed that a much less intense excited-state spectrum is recorded of the complex in acetonitrile or DNA compared to that in water, consistent with formation of the MLCT¹ state in the nonaqueous local environments, characterized by more weakly enhanced resonance Raman scattering. Figure 6A shows subsequent depletion of the MLCT² state over a time range qualitatively consistent with the reported decay time of the species in water.⁴

It was expected that at this 350 nm probe wavelength, it would be possible to utilize the presence of a well-defined band at

1526 cm⁻¹, which previously was observed in nonaqueous environments with a 355 nm probe, to define the progression through states. Indeed, the normalized series of spectra in Figure 4B show a clear shift in the combination of bands close to this position. Spectral subtractions (Figure 5A) were used to determine that this shift was due to the presence of a 1526 cm⁻¹ mode at early times which depleted as conversion to the second state occurred. The nanosecond excited state spectra (Figure 5B) show clear similarities upon subtraction of the spectrum recorded in water from that in acetonitrile, particularly in the prominent 1526 cm⁻¹ feature. The kinetic plot (Figure 6B), which was derived from the measurement of the depletion of the MLCT¹ 1526 cm⁻¹ mode shows good agreement with the series of spectra probed with the 390/390 nm combination, where the kinetics derived from measurement of the grow-in of the 1366 cm⁻¹ feature of the MLCT² species, indicate completion of the conversion within 20 ps. Subtractions were also very useful in determining, as for the 390/390 nm spectra, that further conversion to other species did not take place beyond 20 ps.

We have therefore a sound basis for correlating the present data, recorded in the picosecond time regime, with the proposal based upon previous measurements on the nanosecond time scale that the 1526 cm⁻¹ mode is indicative of resonance with the earlier MLCT¹ state proposed by Barbara et al., i.e., the present results show that ultrafast TR³ can follow the progression of the photophysical decay of the excited complex from the MLCT¹ state, which is marked by the 1526 cm⁻¹ feature, to MLCT² in which this feature is not enhanced.

The regional assignment of the dppz⁻ bands on the basis of the ground-state RR and nanosecond transient RR spectra of a series of deuterated analogues of **1**,^{14b} shows that the 1526 cm⁻¹ band may be attributed to a normal mode vibration which has more "phen-based" character, i.e., enhancement of this feature may be interpreted in terms of resonance with a dppz⁻ intraligand electronic transition of an MLCT state which has increased charge density on the phen segment of the reduced ligand. Thus, if the appearance of the 1526 cm⁻¹ feature can be correlated with the MLCT¹ state, then it may be further

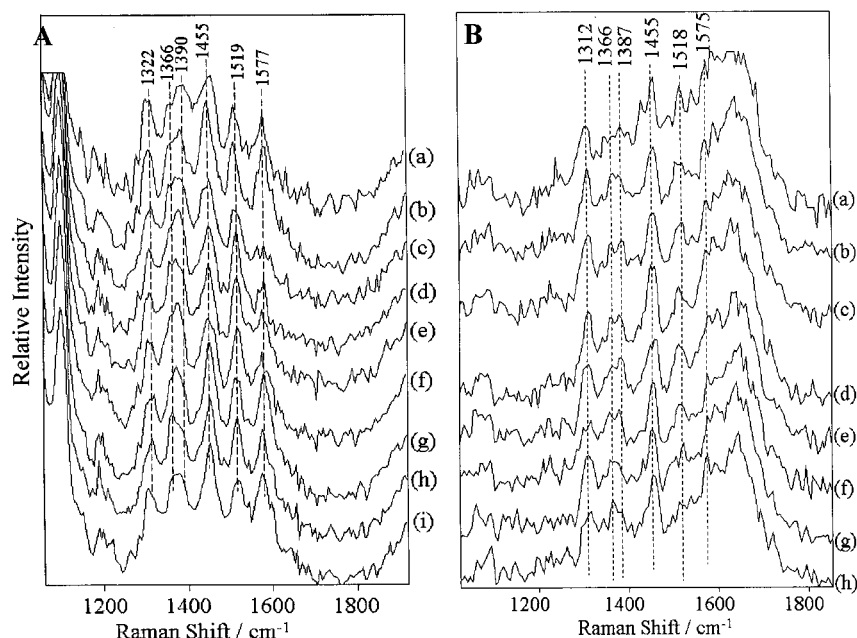


Figure 10. A: Pure excited-state picosecond-TR³ spectra of **1** in *d*₃-acetonitrile at 420 nm pump/420 nm probe time delays of (a) 4, (b) 7, (c) 10, (d) 20, (e) 30, (f) 50, (g) 100, (h) 500, and (i) 1500 ps. B: pure excited-state picosecond-TR³ spectra of **1** with DNA, [DNA phosphate]:[Ru] ratio of 10:1, at 420 nm pump/420 nm probe time delays of (a) 4, (b) 7, (c) 10, (d) 20, (e) 30, (f) 50, (g) 100, and (h) 500 ps.

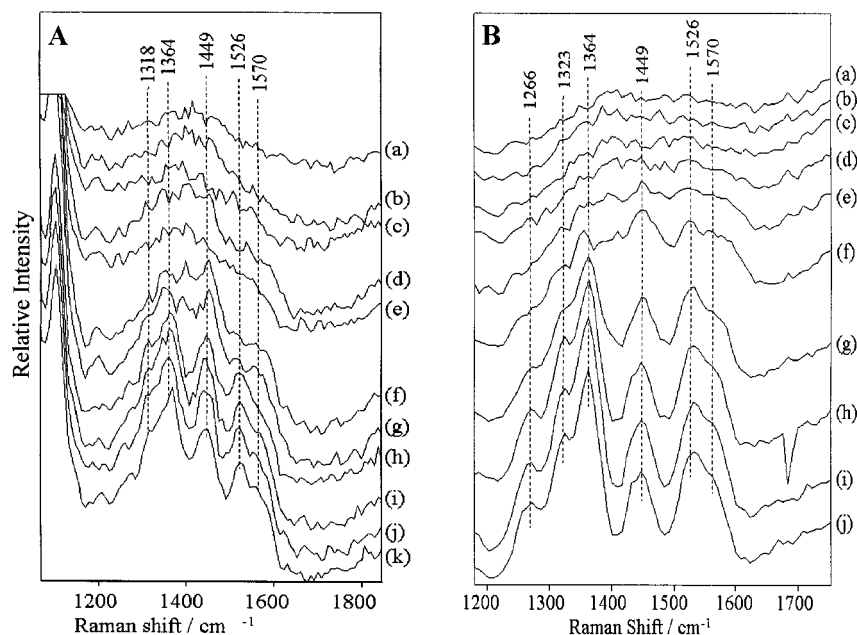


Figure 11. A: Pure excited-state picosecond-TR³ spectra of **1** in d_3 -acetonitrile at 400 nm pump/350 nm probe time delays of (a) 0, (b) 1, (c) 2, (d) 4, (e) 6, (f) 10, (g) 20, (h) 50, (i) 100, (j) 200, and (k) 500 ps. B: pure excited-state picosecond-TR³ spectra of **1** in d_4 -methanol at 400 nm pump/350 nm probe time delays of (a) 0, (b) 2, (c) 4, (d) 6, (e) 10, (f) 20, (g) 50, (h) 100, (i) 200, and (j) 500 ps.

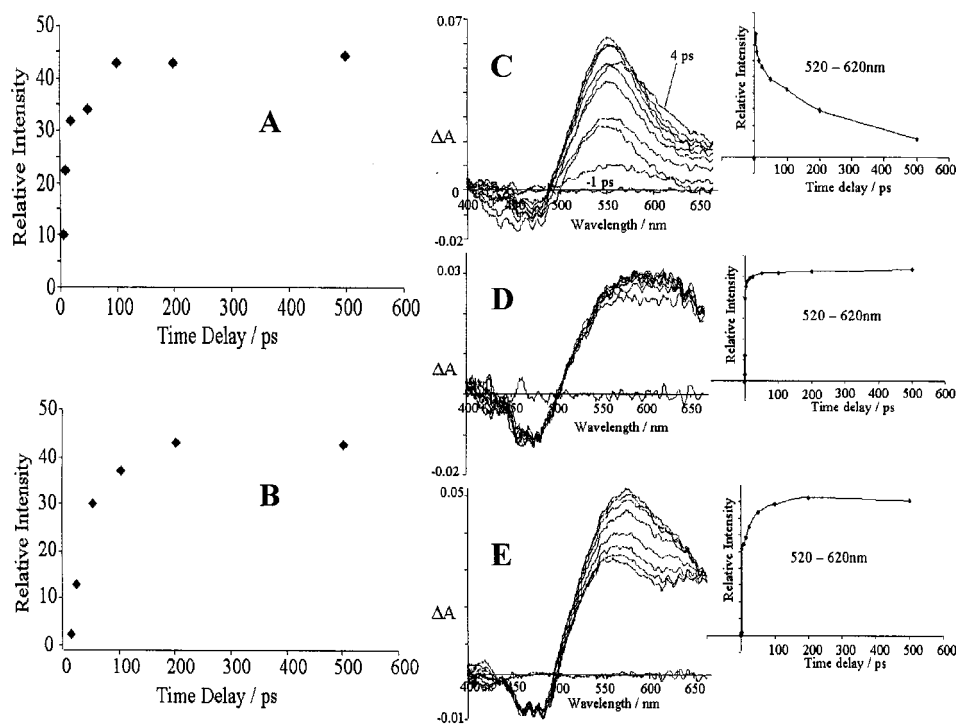


Figure 12. A: kinetics of **1** in acetonitrile at 400 nm pump/350 nm probe, derived from spectra of Figure 11A, plotting relative intensity of 1366 cm^{-1} feature vs time delays between 0 and 500 ps. B: kinetics of **1** in methanol, derived from spectra of Figure 11B. For comparison, C, D, and E show picosecond-transient absorption spectra and corresponding kinetic plots of **1** in water, acetonitrile, and methanol respectively (adapted from ref 19).

proposed that this state is characterized by an electron density which is polarized more toward the phenanthroline segment of the dppz ligand, compared to the MLCT² state, for which no enhancement of the 1526 cm^{-1} feature is observed. This in turn is consistent with a model involving increased stabilization in the polar water environment,^{4,5} of the MLCT² state, which has been proposed to have more electron density on the “phenazine” nitrogens, relative to MLCT¹, and which would facilitate efficient nonradiative decay to the ground state.

The wavelengths used to probe the excited states of **1** in aqueous environment have each yielded a series of TR³ spectra from which it may be estimated that the interconversion time for the process MLCT¹ to MLCT² lies somewhere in the range 5–10 ps, somewhat longer than but not seriously at variance with the 3–4 ps estimated by Barbara et al.⁴ and the Gothenburg group.⁸ Such a relatively long time constant for interconversion between two closely related MLCT states would be consistent with the suggested involvement of a slower, rate-determining

step such as hydrogen bond formation/reinforcement,⁴ or reorientation of strongly hydrogen-bonded water.⁸

[Ru(phen)₂dppz]²⁺ in Nonaqueous Environment. The TR³ studies of **1** in acetonitrile and methanol using probe wavelengths at 390, 420, and 350 nm (Figures 7, 10, and 11) have all provided evidence for the grow-in of a triplet MLCT state which is characteristic of that which has been probed in nanosecond single-color RR experiments. The strongest evidence for this lies in the grow-in of a 1526 cm⁻¹ band which, not unexpectedly, is markedly more enhanced in the 350 nm spectra. Within the ps time range studied, there is no apparent decay from this state, which may be attributed to the MLCT¹ state proposed in the model by Barbara et al. Moreover, with regard to spectra recorded at a probe wavelength of 350 nm, although it is the case in both aqueous and nonaqueous environments that an increase in overall spectral intensity is observed with increasing time delay, it should be noted that the early time delay spectra (~4 ps) in aqueous environment are of comparable relative intensity to the later time delay spectra (>50 ps) in nonaqueous environment. This is a further indication that resonance occurs through the same electronic state, MLCT¹, in both media. Thus, as mentioned earlier, it appears that the scattering due to the MLCT¹ state is enhanced significantly less at 350 nm compared to the MLCT² state, which yields a considerably enhanced spectrum at later time delays in aqueous environment.

An additional feature in the present series of experiments, which was apparently not reported by Barbara et al., arises upon consideration of the spectra in nonaqueous environment. The difference in the enhancement pattern at early times in the 390/390 nm and 420/420 nm spectra is indicative of a "precursor" state which precedes the expected MLCT¹ state. Subtractions have shown (Figure 8) that the early time spectra exhibit some differences compared to the spectra of the charge transfer states. Although in the studies using the 350 nm probe wavelength, the spectra at early times in the acetonitrile and methanol series are dominated by noise, this in itself is informative. It suggests that the precursor state is apparently not in resonance at 350 nm, but that it can be probed at 390 nm. This contrasts with the situation for the MLCT¹ and MLCT² states which are, if anything, more in resonance at this wavelength. Although this suggests that the latter are distinct from the precursor state, we have insufficient information to define its precise nature (vide infra).

It should also be noted that a photophysical model for the light-switch effect has recently been proposed by Benniston et al.,¹⁵ based on some preliminary picosecond RR investigations of [Ru(bpy)₂dppz]²⁺, in various solvents. These workers suggested that the feature at ca. 1390 cm⁻¹, for the complex in acetonitrile, is a solvent-shifted mode and assigned it as the *same mode* which is observed at 1366 cm⁻¹ in aqueous environment, but which we have also observed in the present study for **1** in nonaqueous environments. They explained the shift to higher wavenumber by invoking a "hybrid excited-state model", considered to incorporate characteristics of ³MLCT and triplet-dppz states, suggesting predominance of an excited state in acetonitrile which contained more phenazine-localized triplet character. This distinction in excited states in each environment was proposed by them to be directly linked to the light-switch effect. However, the studies on which these conclusions are based involved pump-probe time delays that did not extend beyond 20 ps. As now demonstrated, the 1366 cm⁻¹ band remains a predominant feature in the acetonitrile environment at times beyond 20 ps, and indeed in the nanosecond RR spectra

in the same environment. Thus, in view of these new findings, it is clear that a dynamic conversion process is taking place between two species individually characterized by bands at 1390 and 1366 cm⁻¹, and we conclude that the two bands cannot be due to the same mode shifted by solvent.

Returning to the proposal of a precursor state, the kinetics of conversion from precursor to MLCT¹ appear to be relatively long in acetonitrile. Such a conversion time would tend to rule out the possibility that it is due to a solvent reorganization, particularly since acetonitrile would be expected to have one of the most rapid solvent responses of all those investigated here.¹⁷ Of possible significance is the fact that the bands in the subtraction spectrum in Figure 8 (lower traces) show some similarities to the nanosecond spectra previously recorded of the complex [Re(CO)₃Cl(dppz)]¹⁸ for which it is known the dppz-based triplet state is the lowest excited-state species. Also the trend with wavelength in resonance enhancement pattern of the state would suggest a greater absorption toward longer wavelengths, as opposed to the charge transfer states where the absorption maximizes near 350 nm. [Re(CO)₃Cl(dppz)] has a transient absorption spectrum with a maximum at ca. 460 nm.¹⁸ While these are points to be taken into consideration, we do not believe they constitute definitive evidence of a triplet state in the case of the precursor, and we would not therefore wish to rule out the possibility that the state is MLCT in character.

The experiments conducted for the complex in methanol, for which the excited-state emissive lifetime has been reported as ca. 45 ns⁵ provide a useful parallel with the studies in acetonitrile. Again, the predominant species in the decay process is shown to be the MLCT¹ state, for which the 1526 cm⁻¹ band is strongly enhanced, particularly at a probe wavelength of 350 nm. The same bands that we have attributed to a precursor state are again observed using a 390/390 nm pump and probe combination. The conversion time from precursor to MLCT¹ appears to be somewhat longer than for the complex in acetonitrile, as seen from a comparison of the kinetic plots in Figure 12A,B.

However, while the existence of a precursor state is evident from the data its precise nature remains unclear at this stage. Furthermore, given that we can clearly identify Raman spectral signatures associated with the specific states (namely, MLCT¹ and MLCT²) at longer times and these states correlate with the "light-switch" phenomena, we do not believe these early time dynamics involving the precursor state play a role in activating/deactivating the "light switch".

Transient Absorption Studies. The early dynamics of **1** are certainly extremely intricate and recent findings from femtosecond TA investigations by the Gothenburg group⁸ of several species containing the [Ru(phen)₂dppz]²⁺ chromophore, (i.e., **1**), as well as some picosecond transient absorption (picosecond-TA) studies on **1** in various solvent environments, carried out by the Belfast group,¹⁹ highlight several complexities. Referring first to the latter studies, transient absorbance difference spectra (ΔA) were recorded with a multichannel diode array detector over the wavelength range 400–700 nm, encompassing both the region of ground-state bleach (~400–500 nm) and the region of excited-state absorption beyond 500 nm. Time delays spanning a 4–500 ps range between pump and continuum probe were employed and the recorded spectra for the complex in water, acetonitrile, and methanol environments are shown for convenience in Figure 12, parts C, D, and E, respectively. Clear differences in the absorption profiles of the dominant excited states of the complex were observed between aqueous and nonaqueous environments. The spectra in aqueous environment

exhibited a positive absorption band which maximized at ca. 575 nm and fell off in intensity significantly toward the lower energy side, a profile typical of triplet MLCT states of a Ru-polypyridyl complex.²⁰ However, while the presence of a region of absorption beyond 500 nm in both acetonitrile and methanol is also suggestive of a ³MLCT state, it extended much further to the red than would normally be expected, pointing to the presence of a distinct state. Significantly, the earliest time delay spectrum of **1** in an aqueous environment showed evidence of additional absorption at the lower energy edge of the profile, again pointing to the likelihood of a second MLCT state. These observations are consistent with picosecond-TR³ results, with both techniques seen to provide independent evidence for two distinct, environment-sensitive ³MLCT states of **1**. Kinetics derived from the picosecond-TA spectra recorded in aqueous solution are also informative,¹⁹ indicating rapid formation of a MLCT state which subsequently decayed over a time range <500 ps, in satisfactory agreement with the 250 ps decay time proposed by Barbara et al.⁴ and the similar value deduced from the present TR³ studies for decay of the MLCT² state. In contrast, corresponding TA data recorded of **1** in nonaqueous environment did not exhibit any decay over the time delays probed. Significantly, however, grow-in of the transient absorption signal in this case showed a time lag in contrast to the virtually instantaneous growth in aqueous environment. Figure 12D,E show that in acetonitrile the grow-in time is 80–100 ps, and ca. 200 ps in methanol, values which correlate very well with kinetics derived from 350/400 nm picosecond-TR³ studies of **1** in nonaqueous solvents, shown in Figure 12A,B. Moreover, these findings may also be interpreted in terms of conversion from a precursor state to MLCT¹. In the TA studies the conversion appears as a grow-in, reflecting a lower absorption for the precursor state in the region beyond 500 nm, compared to the subsequent MLCT¹ state. As a check on the instrumental rise time, picosecond-TA spectra were recorded of the complex $[\text{Ru}(\text{bpy})_3]^{2+}$ in acetonitrile over the same time scale, from which a much more rapid rise in the absorbance beyond 500 nm was observed, exhibiting no further decay over the time range investigated, consistent with the well-established lifetime (in the 100s of nanoseconds range) of the ³MLCT state of this complex.²¹

We now turn to the femtosecond-TA studies⁸ of **1**, and of monomeric and dimeric species containing **1** as the primary chromophore. Although the study largely focused on the monomer and dimer species, it is informative to examine our current findings in light of this investigation, carried out on a much shorter time scale. Following excitation of **1** at 502 nm, toward the red end of the lowest energy MLCT band, two short-lived processes for the complex in water, 0.7 ps and ca. 3 ps, were identified at several probe wavelengths in the range 566–644 nm, the shorter of which exhibited a relatively large change in anisotropy. A slower process was reported also, the lifetime of which is in agreement with that reported by Barbara et al., ~260 ps, representing deactivation from the lowest excited state of **1**. The relatively large anisotropy change of the 0.7 ps process was proposed to be associated with a significant interligand charge redistribution, strongly coupled to the field of surrounding water dipoles. The possible nature of this process is considered further below.

Concerning the second, slower process (3 ps), which was visible in the isotropic absorption signal and less so in the anisotropy, it was pointed out that this had essentially the same time constant (ca. 4ps) as that for reorientation of strongly hydrogen bonded water. While this was taken to be indicative

of rate-limiting solvent reorientation, it was suggested the total process might involve enhancement of hydrogen bond interactions between water and the N lone pairs of the phenazine part of the dppz[−] radical anion, bringing the latter to a PE minimum, as similarly invoked in the Barbara model, which proposes hydrogen bond formation between water and the MLCT¹ state as a rate-limiting equilibration step. While we cannot rigorously exclude the possibility that the difference in MLCT¹ and MLCT² is largely one of differing degrees of solvation, the TR³ evidence presented here, along with additional results on deuterated forms of **1** (not shown here¹⁴), points strongly in favor of two distinct states with differing localizations of the electron density. Moreover, the differences in the picosecond transient absorption spectra in water and acetonitrile (Figure 12C,D above) are also supportive of this.

Returning to the question of the faster, strongly anisotropic process in water, it is interesting to consider the possibility that it is analogous to the markedly longer (ca. >30 ps) initial conversion process observed in nonaqueous environments (Figure 12), the process being much too short-lived in water (0.7 ps) to be detected by our picosecond-TR³ or picosecond-TA experiments. This would require the early time process, involving the aforementioned “precursor” state, to be very sensitive to the local environment. Indeed we have already drawn attention to the apparent solvent dependence of the process, which appears to be somewhat slower in methanol compared to acetonitrile, suggesting that the lifetime of the process may be inversely related to the dielectric constant of the medium. The markedly higher dielectric constant of water might well impose a subpicosecond time scale on the process.²²

The fundamental question remains regarding the nature of the photophysical interaction of **1** bound to DNA, and the femtosecond studies⁸ were extended to address this issue. Here, two early time processes were uncovered, exhibiting lifetimes of 7 and 37 ps, with no evidence of a subpicosecond process. Probing at 574–644 nm, the change was more prominent in the anisotropy than in the TA. These processes were ascribed to “a change of the structural and electronic equilibration in the DNA intercalation pocket”, suggesting that the “solvation” process might involve structural rearrangement of the DNA binding pocket as well as changes of the location of the metal complex in it. However, in light of the findings from the current picosecond-TR³ studies, an alternative viewpoint merits some examination. There are two points worth consideration: (a) both of the early processes in DNA exhibited comparable changes in anisotropy, whereas in water the faster 0.7 ps process showed a markedly larger anisotropy change compared to the 3 ps process and (b) decay from the intensely emitting MLCT¹ state in DNA environment is bi-/multiexponential,^{1d} in contrast to the situation in acetonitrile where a monoexponential decay is clearly observed. Thus, an alternative explanation for the two anisotropic processes in DNA might be to suggest that they are the counterpart of the anisotropic 0.7 ps process in water, but show biexponential character, in line with the biexponential emissive decay in DNA from the MLCT¹ state. Hence the varying extent of protection afforded to the DNA-intercalated dppz ligand could perhaps be envisaged as providing a local environment for the ligand that varies in viscosity, dielectric, and hydrogen-bonding properties which could account for both the long emission lifetime and for the environment-sensitive early anisotropic process.

Conclusions

Picosecond-TR³ at each pump–probe wavelength combination, has been employed to follow the progression of the

photophysical decay of **1** in aqueous environment. Relevant marker bands and overall spectral intensities have been used to probe the conversion from MLCT¹ to MLCT², which is complete within 20 ps. Further decay from MLCT² is in agreement with the lifetime of ca. 250 ps reported by Barbara et al.

Marker bands such as that at 1526 cm⁻¹, may be used to correlate the present picosecond-TR³ data with earlier measurements by nanosecond-TR². Early time picosecond-TR³ spectra in aqueous environment have similarity to nanosecond-TR² spectra of the complex in nonaqueous environment, whereas later time picosecond-TR³ spectra show similarity to nanosecond-TR² of **1** in aqueous environment. Thus, the ultrafast time resolution has effectively probed at early time (<20 ps), the MLCT¹ state which may only be probed in nonaqueous environment (in which it is the dominant state) by nanosecond-TR².

In aqueous environment, spectral subtractions have been effective in confirming only two phases of decay *within the available time-resolution*, i.e., MLCT¹ to MLCT² to ground state.

Picosecond-TR³ experiments have confirmed that the prominent (thermally equilibrated) excited state of **1** in nonaqueous environment can be identified as the earlier state in aqueous environment, i.e., MLCT¹.

In a slight departure from the Barbara photophysical model, picosecond-TR³ spectra have provided evidence of a "precursor excited state" which precedes the MLCT¹ state, is reasonably distinct in nature from the MLCT states, and is probed within the present time-resolution in nonaqueous environment only. This state, while itself exhibiting a solvent-dependent lifetime, is not considered to participate directly in the *light-switch* mechanism.

The lifetime of the precursor state is possibly inversely related to the dielectric constant of the solvent environment, apparently becoming subpicosecond in the high dielectric medium of water. There is a likely correlation between the precursor state and the 0.7 ps state of **1**, which exhibits considerable anisotropy change, as reported recently on the basis of femtosecond-TA measurements.⁸

The present picosecond-TR³ findings show excellent agreement with picosecond-TA experiments with a multichannel detector,¹⁹ performed in parallel with the present study. The picosecond-TA studies provided independent evidence of (a) a distinction in TA profile between MLCT¹ and MLCT² states, (b) decay from MLCT² in nonaqueous environment with a lifetime of ca. 250ps, and (c) solvent-dependent grow-in of the MLCT¹ state from the precursor state in nonaqueous environment.

Acknowledgment. The Belfast group thanks the EPSRC for support, including access to the Laser Facility at RAL, and for the provision of a project studentship to M.C. (Grant GR/M45696). We also thank Dr J. Hamilton for synthetic support and Dr P. Callaghan for discussions. The Gothenburg work was supported by the Swedish Natural Science Research Council (NFR) and experiments at RAL carried out under the EU Access to Large-Scale Facilities Program.

References and Notes

(1) (a) Friedman, A. E.; Chambron, J.-C.; Sauvage, J.-P.; Turro, N. J.; Barton, J. K. *J. Am. Chem. Soc.* **1990**, *112*, 4960. (b) Norden, B.; Lincoln,

P.; Akerman, B.; Tuite, E. *Metal Ions in Biological Systems*; Sigel, A., Sigel, H., Eds.; Marcel Dekker: New York, 1996; Vol. 33, p 177. (c) Kirsch-De Mesmaeker, A.; Kelly, J. M. *Top. Curr. Chem.* **1996**, *177*, 25. (d) Hiort, C.; Lincoln, P.; Norden, B. *J. Am. Chem. Soc.* **1993**, *115*, 3448. (e) Haq, I.; Lincoln, P.; Suh, D.; Norden, B.; Chowdhry, B. Z.; Chaires, J. B. *J. Am. Chem. Soc.* **1995**, *117*, 4788. (f) Lincoln, P.; Broo, A.; Norden, B. *J. Am. Chem. Soc.* **1996**, *118*, 2644. (g) Tysoe, S. A.; Morgan, R. J.; Baker, A. D.; Streckas, T. C. *J. Phys. Chem.* **1993**, *97*, 1707. (h) Choi, S.-D.; Kim, M.-S.; Kim, S. K.; Lincoln, P.; Norden, B. *Biochemistry* **1997**, *36*, 214. (i) Tuite, E.; Lincoln, P.; Norden, B. *J. Am. Chem. Soc.* **1997**, *119*, 239. (j) Marincola, F. C.; Casu, M.; Saba, G.; Lai, A.; Lincoln, P.; Norden, B. *Chem. Phys.* **1998**, *236*, 301. (k) Jenkins, Y.; Friedman, A. E.; Turro, N. J.; Barton, J. K. *Biochemistry*, **1992**, *31*, 10809. (l) Dupureur, C. M.; Barton, J. K. *Inorg. Chem.* **1997**, *36*, 33. (m) Önfelt, B.; Lincoln, P.; Norden, B. *J. Am. Chem. Soc.* **1999**, *121*, 10846. (n) Schoonover, J. R.; Bates, W. D.; Meyer, T. J. *Inorg. Chem.* **1995**, *34*, 6421. (o) Coates, C. G.; Jacquet, L.; McGarvey, J. J.; Bell, S. E. J.; Al-Obaidi, A. H. R.; Kelly, J. M. *J. Am. Chem. Soc.* **1997**, *119*, 7130. (p) Chen, W.; Turro, C.; Friedman, L. A.; Barton, J. K.; Turro, N. J. *J. Phys. Chem. B* **1997**, *101*, 6995.

(2) Takahara, P. M.; Rosenzweig, A. C.; Frederick, C. A.; Lippard, S. J. *Nature* **1995**, *377*, 649. (b) Takahara, P. M.; Frederick, C. A.; Lippard, S. J. *J. Am. Chem. Soc.* **1996**, *118*, 12309.

(3) Coates, C. G.; McGarvey, J. J.; Callaghan, P. L.; Coletti, M.; Hamilton, J. G. *J. Phys. Chem. B* **2001**, *105*, 730.

(4) Olsen, E. J. C.; Hu, D.; Hormann, A.; Arkin, M. R.; Stemp, E. D. A.; Barton, J. K.; Barbara, P. F. *J. Am. Chem. Soc.* **1997**, *119*, 11458.

(5) Nair, R. B.; Cullum, B.; Murphy, C. J. *Inorg. Chem.* **1997**, *36*, 962.

(6) The superscripts "1" and "2" employed in the present paper are equivalent to the superscripts "h" and "l" used in ref 4.

(7) The scheme is qualitatively similar to that used by Barbara et al. in ref 4, but extended somewhat to include a precursor state as proposed in the text. The energy levels shown are entirely qualitative.

(8) Önfelt, B.; Lincoln, P.; Norden, B.; Baskin, J. S. *Zewail, A.H. Proc. Natl. Acad. Sci. U.S.A.* **2000**, *97*, 5708.

(9) Schoonover, J. R.; Strouse, G. F. *Chem. Rev.* **1998**, *98*, 1335.

(10) Coates, C. G.; Callaghan, P. L.; McGarvey, J. J.; Kelly, J. M.; Kruger, P. E.; Higgins, M. E. *J. Raman Spectrosc.* **2000**, *31*, 283.

(11) Towrie, M.; Parker, A. W.; Shaikh, W.; Matousek, P. *Meas. Sci. Technol.* **1998**, *9*, 816.

(12) Matousek, P.; Towrie, M.; Stanley, A.; Parker, A. W. *Appl. Spectrosc.* **1999**, *53*, 1485.

(13) Gordon, K. C.; McGarvey, J. J. *Inorg. Chem.* **1991**, *30*, 2986.

(14) (a) Callaghan, P. L. Ph.D. Thesis, The Queen's University of Belfast, Belfast, 2000. (b) Callaghan, P. L.; Coates, C. G.; McGarvey, J. J.; Kelly, J. M.; Higgins, M. E.; Kruger, P. E. Manuscript in preparation.

(15) Benniston, A. C.; Parker, A. W.; Matousek, P. *J. Raman Spectrosc.* **2000**, *31*, 503.

(16) Pure excited-state spectra of **1** in a 2:1 and 1:1 mixture of H₂O/*d*₃-acetonitrile were recorded with 390/390 nm and 400/350 nm pump and probe combinations at a range of time delays between 4 and 1000 ps. Subtractions based on this series suggest markedly different kinetics of conversion compared to the corresponding situation for the complex in pure water. In general, the kinetics of conversion extended to longer times than in pure water, the later time delay spectra being very representative of the MLCT² state. However, the complex nature of the subtraction studies suggested that the photophysics could not be described by a simple "lengthening" of the water mechanism, possibly due to a heterogeneous solvent mixture inducing more than one mechanism to occur simultaneously within the probed volume.

(17) Stratt, R. M.; Maroncelli, M. *J. Phys. Chem.* **1996**, *100*, 12981.

(18) Waterland, M. R.; Gordon, K. C.; McGarvey, J. J.; Jayaweera, P. M. *J. Chem. Soc., Dalton Trans* **1998**, 609.

(19) Coates, C. G.; Callaghan, P. L.; McGarvey, J. J.; Kelly, J. M.; Jacquet, L.; Kirsch-De Mesmaeker, A. *J. Mol. Struct.* **2001**, *598*, 15.

(20) Coates, C. G.; Keyes, T. E.; Hughes, H. P.; Jayaweera, P. M.; McGarvey, J. J.; Vos, J. G. *J. Phys. Chem. A* **1998**, *102*, 5013.

(21) Balzani, V.; Scandola, F. *Supramolecular Photochemistry*; Ellis Horwood: New York, 1991.

(22) Recent unpublished results by the Gothenburg Group, of femtosecond linear dichroism and transient absorption measurements on **1** in a series of alcohols has described a process with a large anisotropy and with lifetimes in the region of tens of picoseconds. The process shows an inverse relationship with the dielectric constant of the solvent, the shortest lifetime being observed for methanol, which has the highest dielectric constant. Acetonitrile, with a higher dielectric constant than methanol, might reasonably be expected to exhibit a shorter lifetime again.